Fuel Cells

DOI: 10.1002/anie.201005745

Catalytic Reactions in Direct Ethanol Fuel Cells**

In Kim, Oc Hee Han, Seen Ae Chae, Younkee Paik, Sung-Hyea Kwon, Kug-Seung Lee, Yung-Eun Sung, and Hasuck Kim*

For fuel-cell applications, ethanol is becoming a more attractive fuel than methanol or hydrogen because it has higher mass energy density and can be produced in great quantities from biomass.[1] Additionally, ethanol is less toxic than methanol and easier to handle than hydrogen.[2,3] However, the C–C bond in ethanol leads to more complicated reaction intermediates and products during oxidation,[2–12] and catalysts must be able to activate C–C bond scission for complete oxidation to CO_2. Consequently, much effort has been made to investigate the reaction mechanisms of direct ethanol fuel cells (DEFCs) with various analytical methods.[2–12] Especially the intermediates and products that are generated during the electrochemical reaction at different ethanol concentrations and potentials have been investigated and quantified by chromatographic techniques,[4–6] infrared reflectance spectroscopy (IRS),[4,6–9] and differential electrochemical mass spectrometry (DEMS).[8–10] These studies revealed that most of the ethanol was oxidized to acetic acid (AA) or acetaldehyde (AAL) on Pt, but not much to CO_2. Additionally, investigations of ethanol oxidation on various catalysts showed that alloying Pt with other transition elements improves the catalytic activity.[6,10,12,13] However, DEMS is limited to the detection of volatile chemicals, and IRS requires smooth electrodes with sufficient reflectivity. On the other hand, liquid-state nuclear magnetic resonance (NMR) spectroscopy is a straightforward analytical method which can be applied to an operating fuel cell without any modification.[14] In liquid-state NMR spectroscopy, peak areas are linearly proportional to the abundance of chemical species that are identifiable by their chemical shifts. The DEFC anode exhaust has been shown to give well-resolved ^{13}C peaks that can unambiguously identify chemical species.[14] We have used ^{13}C liquid-state NMR spectroscopy to identify and quantify the reaction products present in the liquid anode exhaust of DEFCs that were operated with three different anode catalysts at various potentials. The results were used to explain the effect of elements such as Ru and Sn on the Pt/C anode catalyst and to propose reaction mechanisms of ethanol on Pt-based catalysts.

The ^{13}C liquid-state NMR experiments were performed on DEFCs containing 40 wt% Pt/C, PtRu/C, or Pt_3Sn/C anode catalysts prepared by a polyol method. Full experimental details are described in the Supporting Information. Figure 1 shows the ^{13}C NMR spectra of the anode exhaust from the DEFCs with Pt_3Sn/C anode catalysts. The spectra were expanded in the *y* scale while maintaining the relative peak heights. The chemical species were assigned to the peaks in the spectrum according to literature data,[15] and C atoms that are responsible for ^{13}C NMR signals are underlined. In the exhaust, the dominant reaction products were AAL ($\delta =$ 207 ppm), AA ($\delta = 177$ ppm), and ethane-1,1-diol (ED, $\delta =$ 88 ppm) at various potentials. Ethyl acetate ($\delta = 62, 175$ ppm) and ethoxyhydroxyethane ($\delta = 63,\ 95$ ppm) also appeared, but only in trace amounts and hence were ignored. The coupling constants of 2.8 and 1.6 Hz between the ^{13}C-labeled sites were used to distinguish CH_2 groups in ethyl acetate and ethoxyhydroxyethane, respectively. For comparison purposes, the NMR spectra were also obtained for the DEFCs containing Pt/C and PtRu/C anode catalysts, and AA, AAL, and ED were major products detected for all three catalysts.

Figure 2 shows the relative quantities of the major organic chemicals in the anode exhaust of the DEFCs with different anode catalysts at different potentials. For the DEFC with Pt/C anode catalyst, the NMR peak areas of the reaction products were monotonically depleted with increasing operating potential above 0.1 V versus the standard hydrogen electrode. Thus, more oxidation products were produced from the fuel when the DEFC was operated at a higher current and a lower potential. However, the addition of Ru or Sn to Pt caused variations in the NMR spectral patterns. Production of AA dramatically increased. Subtracting the product populations for Pt/C from those for PtRu/C and Pt_3Sn/C (dotted lines in Figure 2) separates the contributions of Ru or Sn from those due to Pt/C. For example, the enhanced AAL and ED production on PtRu/C and Pt_3Sn/C compared to on Pt/C was almost zero at 0.1 V and slightly increased above 0.2 V. In contrast, AA production was greatly enhanced and different production behaviors were observed depending on the anode catalysts. On the PtRu/C anode catalysts, AA production

[*] Dr. I. Kim,[+] Dr. O. H. Han, Dr. S. A. Chae, Dr. Y. Paik, S.-H. Kwon
Analysis Research Division, Daegu Center
Korea Basic Science Institute, Daegu, 702-701 (Korea)
Fax: (+82) 53-959-3405
E-mail: ohhan@kbsi.re.kr
Dr. O. H. Han
Graduate School of Analytical Science and Technology
Chungnam National University, Daejeon, 305-764 (Korea)
Dr. I. Kim,[+] Dr. H. Kim
Department of Chemistry, Seoul National University
Seoul, 151-747 (Korea)
Dr. K.-S. Lee,[$] Dr. Y.-E. Sung
School of Chemical and Biological Engineering
Seoul National University, Seoul, 151-744 (Korea)
[+] Present address: SB LiMotive Co., Ltd., Yongin (Korea)
[$] Present address: Fuel Cell Center, Korea Institute of Science and Technology, Seoul (Korea)

[**] This work was supported by KBSI grants (K29030 and K30030) to O.H.H.

Supporting information for this article is available on the WWW under http://dx.doi.org/10.1002/anie.201005745.

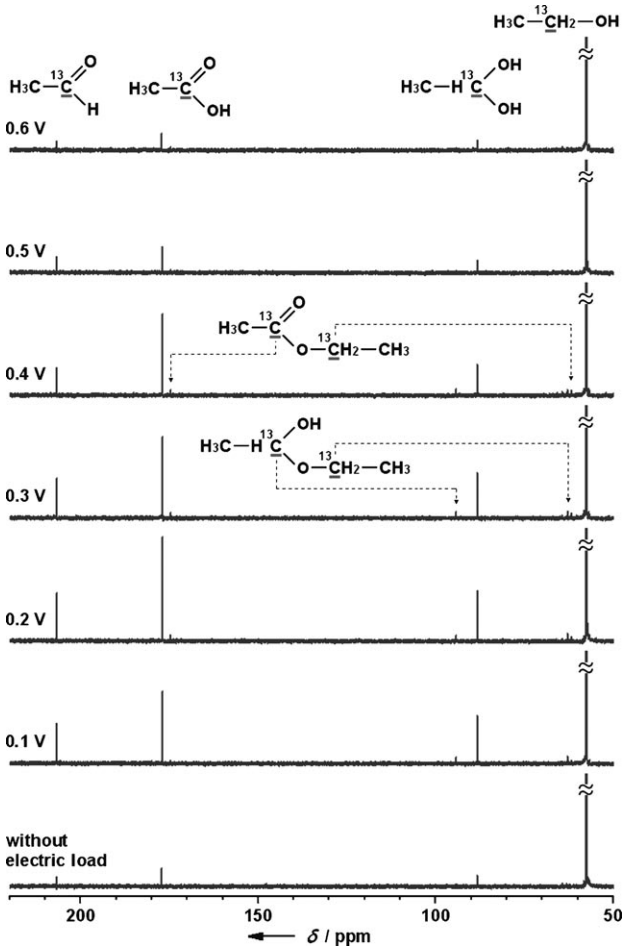

Figure 1. Representative ^{13}C liquid-state NMR spectra of the anode exhaust collected at different operation potentials for a DEFC containing 40 wt% Pt_3Sn/C anode catalyst.

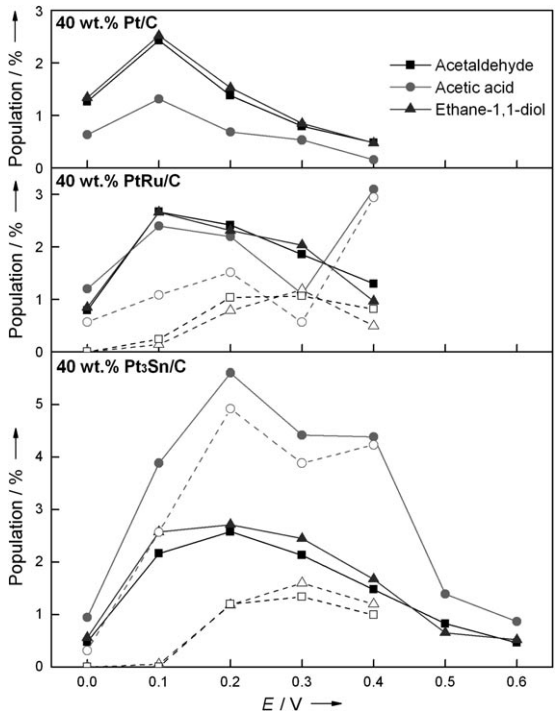

Figure 2. Populations of the reaction products in the anode exhaust versus operating potential of fuel cells containing Pt/C, PtRu/C, or Pt_3Sn/C anode catalyst. The dotted lines indicate the populations of the reaction products versus operating potential after subtracting the values of the fuel cell with Pt/C anode catalyst.

drastically increased at 0.4 V. On the other hand, AA production was dominant on Pt_3Sn/C over a wider potential range and reached a maximum at 0.2 V.

The electric energy that is stored in an ethanol molecule can be regarded as $12\,e^-$ according to Equation (1).

$$C_2H_5OH + 3\,H_2O \rightarrow 2\,CO_2 + 12\,H^+ + 12\,e^- \quad (1)$$

However, conversion of ethanol into CO_2 is rather low in DEFCs.[4,5,7,10] In reality, AAL and AA were the major oxidation products,[4,5,7,10] and ED was also a major product detected by NMR spectroscopy in this study. Therefore, the amounts of the individual products reflect the reaction pathways and the effectiveness of the catalysts. Energy corresponding to $2\,e^-$ is converted during generation of single AAL or ED molecules, while $4\,e^-$ are converted in the generation of single AA molecules, as summarized in Equations (2)–(4).

$$CH_3CH_2OH \rightarrow CH_3CHO + 2\,H^+ + 2\,e^- \quad (2)$$

$$CH_3CH_2OH + H_2O \rightarrow CH_3CH(OH)_2 + 2\,H^+ + 2\,e^- \quad (3)$$

$$CH_3CH_2OH + H_2O \rightarrow CH_3COOH + 4\,H^+ + 4\,e^- \quad (4)$$

Additionally, these equations show that the production of AA and ED, but not AAL, may be greatly influenced by the reaction of water on the catalysts. In fact, oxygenated species, such as OH, that were adsorbed on the catalysts from the reaction of water, influence the oxidation of CO-like species on PtRu or Pt_3Sn catalysts.[6,12,13,16] The potential dependences of the water reaction and adsorption-site competition between water and fuel or its reaction intermediates were reported.[2,6] Therefore, the drastically increased production of AA at 0.4 V on PtRu/C might be due to enhanced reaction of water with reaction intermediates, such as $-COCH_3$, that were adsorbed on the surface of the catalysts (Scheme 1). However, ED, which may be similarly influenced by the water reaction, did not behave in the same manner as AA with respect to the quantity produced at various potentials. The potential dependence of the enhanced ED population on Pt_3Sn/C or PtRu/C behaved differently from that of the enhanced AA population and was very similar to that of the enhanced AAL population. These different behaviors of ED and AA production clearly indicate that not only the water dissociation reaction but also other factors that affect all of the pre-reactions in Scheme 1 are controlling factors for generation of the reaction products. Thus, the potential dependences of all of the reaction-controlling parameters, such as the adsorption strength of the reaction intermediates[3,6,12,16] and the water reaction,[6,12,13,17] are expected to differ for each catalyst. Another possible explanation is that

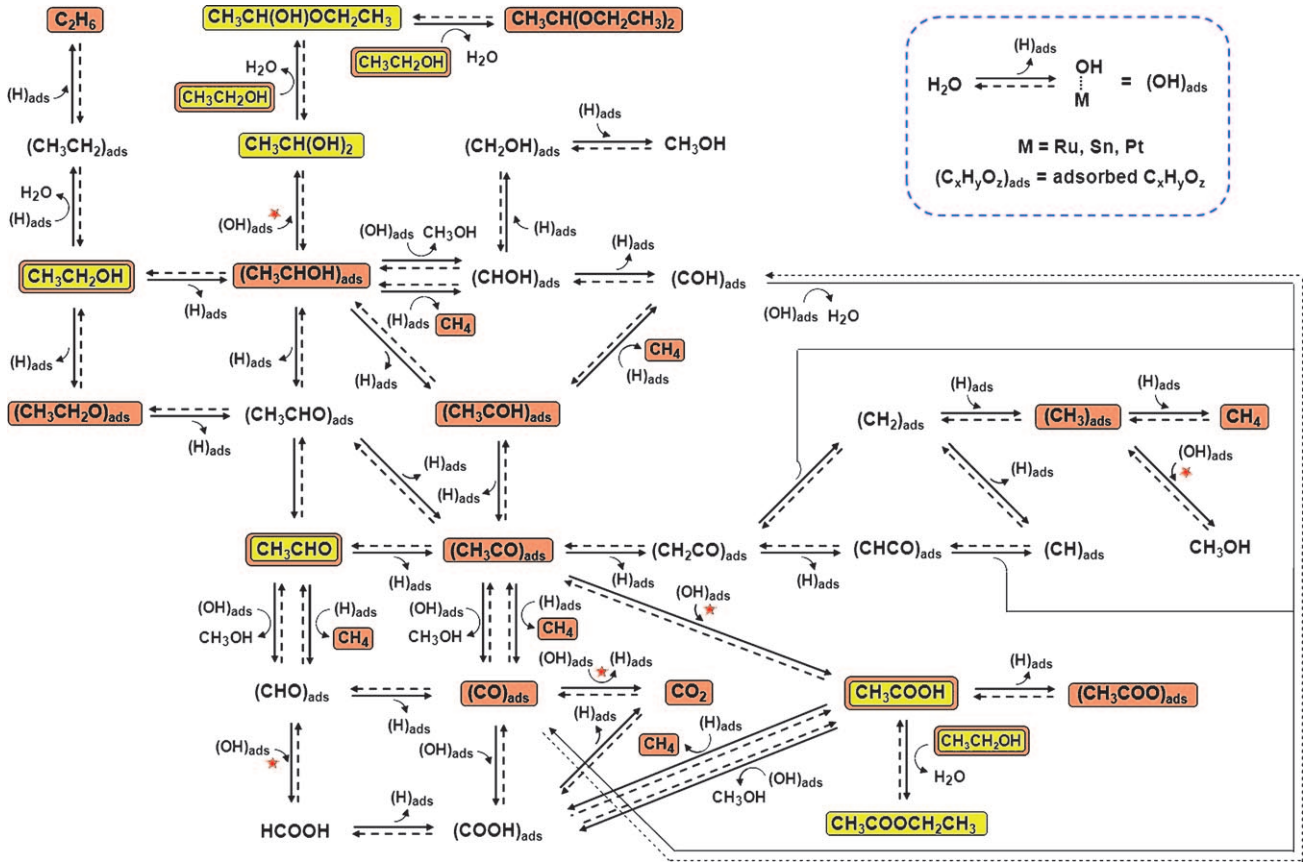

Scheme 1. Ethanol electrochemical reaction pathways on Pt-based catalysts, proposed on the basis of our NMR data and previous reports.[2–13,17–20] See text for detailed explanation. The reaction steps marked with red stars are those in which adsorbed hydroxy groups $(OH)_{ads}$ are involved and catalytic sites are regenerated due to reaction with $(OH)_{ads}$. The chemical species highlighted in yellow were observed in this study, and those highlighted in brown in previous studies using other analytical techniques.

ED and AAL are intermediates to be converted into AA. On the other hand, AA behaved like a final product in this case. In fact, in Figure 2 the overall patterns of the increased amounts of AA, AAL, and ED (similar amounts and leveling of the enhanced production of AAL and ED at potentials above 0.2 V, and the wider variation in the enhanced AA production versus the potential) also suggest that AAL and ED are not final products but intermediates to be converted into AA, even in the presence of enhanced reaction activity due to Sn or Ru.

For integrated interpretation of the catalytic reactions, the NMR results were correlated with electrochemical characterization of the catalysts, such CO-stripping voltammetry[16] and linear-sweep voltammetry of ethanol oxidation in Figure 4, and the unit cell performance (Figure S4, Supporting Information). The onset potential of 0.41 V for CO stripping with PtRu/C catalyst was lower than that of 0.65 V for Pt/C and was consistent with the enhanced AA production at 0.4 V for PtRu/C. Compared to the Pt/C and PtRu/C catalysts, the onset potential and peak width of the Pt_3Sn/C catalyst were lower and broader in the voltammetric data for CO stripping[16] and ethanol oxidation. The current and power also increased for the Pt_3Sn/C catalyst in the unit cell performance (Figure S4, Supporting Information), resulting in more efficient ethanol oxidation on Pt_3Sn/C compared to PtRu/C or Pt/C (Figure 3). Comparison of the NMR results and the electrochemical data indicated that the current density was

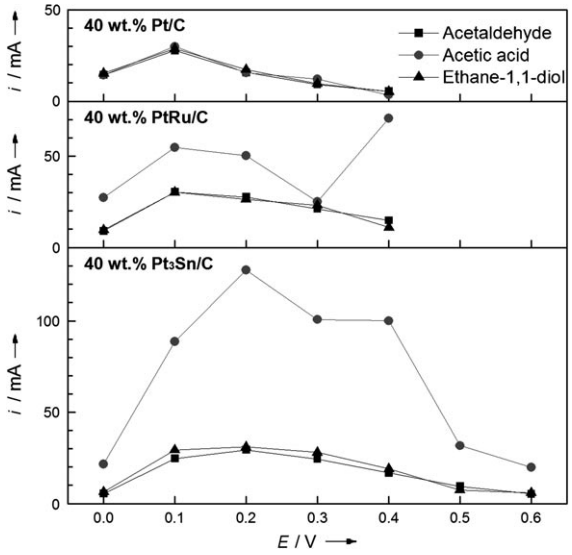

Figure 3. Current generated from each reaction product in the anode exhaust versus operating potential of fuel cells containing Pt/C, PtRu/C, or Pt_3Sn/C anode catalysts.

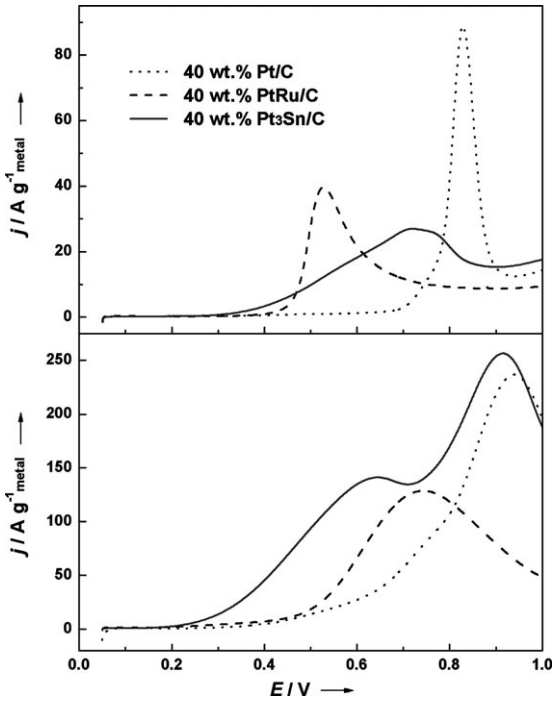

Figure 4. CO-stripping voltammograms (top) and linear-sweep voltammograms for ethanol oxidation (bottom) on each catalyst.

enhanced after adding Sn or Ru to Pt/C because of increased AA production, which was strongly dependent on the potential and the metal that was added to Pt/C. Over a wider potential range and at the lower onset potential than on the other catalysts, the present NMR data for enhanced AA production on Pt_3Sn/C catalyst are consistent with the CO-stripping and linear-sweep ethanol-oxidation voltammetry data. The onset potential for the CO-stripping and/or ethanol-oxidation voltammetry agreed with the potential at which the enhanced AA population reaches a maximum for Pt_3Sn/C or PtRu/C, and corresponds to the optimal population and distribution of the oxygenated species, such as OH, that were adsorbed on the Pt_3Sn/C or PtRu/C catalysts for AA production at the onset potential.

In Scheme 1, in the initial steps of the ethanol adsorption and oxidation, ethanol is adsorbed on Pt as Pt–OCH_2–CH_3 and Pt–CHOH–CH_3, as reported previously.[6,9,18] Once intermediate species such as Pt–CO–CH_3 and Pt–CO are formed, they are oxidized to CH_3COOH or CO_2 by reaction with an oxygen-containing species, such as OH, from the dissociative adsorption of water on Ru, Sn, and Pt.[5,6,13,19,20] CO species on Pt were detected by FTIR spectroscopy,[4,6–9] and some traces of CH_4 and CH_3CH_3 were detected in previous studies.[4,9,17] In this NMR study, the main products, AA, AAL, and ED, were detected with minor products such as $CH_3COOCH_2CH_3$ and $CH_3CH(OH)OCH_2CH_3$ produced in homogeneous reactions. $CH_3CH(OCH_2CH_3)_2$ is expected to be produced by a homogeneous reaction between ethanol and $CH_3CH(OH)OCH_2CH_3$ when the concentration of $CH_3CH(OH)OCH_2CH_3$ is high. The ethanol reaction pathways in Scheme 1 are proposed by combining all of the above results. The major pathways from ethanol to AA are expected to vary with the anode catalyst and experimental conditions, such as operating potential and temperature. The major pathways under any particular conditions can be studied kinetically and/or by observing intermediates adsorbed on the catalysts.

The present NMR method, which examined the chemicals in the liquid exhaust from the anode, could not be used to detect the chemical species that were adsorbed on the catalysts or gas-phase products such as CO_2, CH_4, and CH_3CH_3. However, generation of these gas-phase products was insignificant[4,5,7,10,17] and the products in the liquid exhaust were in semi-equilibrium with the adsorbed species on the catalysts. Quantitative analyses of the reaction products, as demonstrated in this study, will provide information that can be used to overcome the hindrances to the commercialization of fuel cells. The variation parameters for the analyses include fuel-cell operating conditions such as potential, fuel concentration, and reagent flow rates. Fuel cells that are prepared with different components such as catalysts or electrolyte membranes can also be analyzed. The quantitative analyses also can supply data for more detailed theoretical studies of reaction intermediates and products in the fuel cells.[4,6]

In summary, the dependence of product populations on potential, measured by NMR spectroscopy, is clearly different on each catalyst, especially for AA. The increased current of the DEFCs that were prepared with the Pt_3Sn/C or PtRu/C anode catalyst was mainly due to enhanced production of AA, which was the greatest for Pt_3Sn/C. ED is a major product detected by NMR spectroscopy in addition to the previously reported major products AA and AAL. With the maximum AA population for Pt_3Sn/C or PtRu/C, the potentials were consistent with the onset potentials of CO-stripping and ethanol-oxidation voltammetry. The different dependences on potential for AA and ED production suggest that the water dissociation reaction was not the only major controlling factor for the AA and ED production, and AAL and ED behave as intermediates to be converted into AA. All products that were identified in the liquid exhaust by NMR spectroscopy in this study and previous reports on ethanol oxidation led to the proposed ethanol reaction pathways. The NMR experiments demonstrated here can be carried out in a much shorter time with probes that are equipped with smaller NMR coils[21] and better sensitivities. The NMR analyses can be performed on-line and automated if the fuel cell is adapted to an LC-NMR-type spectrometer.[22] In terms of hardware, integrating the NMR analyses with other on-line analyses such as differential electrochemical mass spectrometry (DEMS) and in situ FTIR of the reaction products in an operating fuel cell could be highly desirable to improve investigation of the fuel-cell reaction mechanism.

Received: September 14, 2010
Revised: November 11, 2010
Published online: February 8, 2011

Keywords: electrochemistry · ethanol oxidation · fuel cells · NMR spectroscopy · reaction mechanisms

[1] A. Demirbas, *Prog. Energy Combust. Sci.* **2007**, *33*, 1.
[2] C. Lamy, A. Lima, V. LeRhun, F. Delime, C. Coutanceau, J.-M. Léger, *J. Power Sources* **2002**, *105*, 283.
[3] S. Song, P. Tsiakaras, *Appl. Catal. B* **2006**, *63*, 187.
[4] H. Hitmi, E. M. Belgsir, J.-M. Léger, C. Lamy, R. O. Lezna, *Electrochim. Acta* **1994**, *39*, 407.
[5] S. Q. Song, W. J. Zhou, Z. H. Zhou, L. H. Jiang, G. Q. Sun, Q. Xin, V. Leontidis, S. Kontou, P. Tsiakaras, *Int. J. Hydrogen Energy* **2005**, *30*, 995.
[6] F. Vigier, C. Coutanceau, F. Hahn, E. M. Belgsir, C. Lamy, *J. Electroanal. Chem.* **2004**, *563*, 81.
[7] G. A. Camara, T. Iwasita, *J. Electroanal. Chem.* **2005**, *578*, 315.
[8] J. P. I. de Souza, S. L. Queiroz, K. Bergamaski, E. R. Gonzalez, F. C. Nart, *J. Phys. Chem. B* **2002**, *106*, 9825.
[9] T. Iwasita, E. Pastor, *Electrochim. Acta* **1994**, *39*, 531.
[10] H. Wang, Z. Jusys, R. J. Behm, *J. Power Sources* **2006**, *154*, 351.
[11] A. F. Lee, D. E. Gawthrope, N. Hart, K. Wilson, *Surf. Sci.* **2004**, *548*, 200.
[12] H. Li, G. Sun, L. Cao, L. Jiang, Q. Xin, *Electrochim. Acta* **2007**, *52*, 6622.
[13] M. Watanabe, S. Motoo, *J. Electroanal. Chem.* **1975**, *60*, 275.
[14] Y. Paik, S.-S. Kim, O. H. Han, *Electrochem. Commun.* **2009**, *11*, 302.
[15] C. Pouchert, J. Behnke, *The Aldrich Library of ^{13}C and ^{1}H FT-NMR Spectra*, Aldrich, St. Louis, **1993**.
[16] D. Lee, S. Hwang, I. Lee, *J. Power Sources* **2005**, *145*, 147.
[17] V. M. Schmidt, R. Ianniello, E. Pastor, S. Gonázlez, *J. Phys. Chem.* **1996**, *100*, 17901.
[18] R. A. Rightmire, R. L. Rowland, D. L. Boos, D. L. Beals, *J. Electrochem. Soc.* **1964**, *111*, 242.
[19] Y. Morimoto, E. B. Yeager, *J. Electroanal. Chem.* **1998**, *441*, 77.
[20] T. E. Shubina, M. T. M. Koper, *Electrochim. Acta* **2002**, *47*, 3621.
[21] R. Subramanian, M. M. Lam, A. G. Webb, *J. Magn. Reson.* **1998**, *133*, 227.
[22] F. Xu, A. J. Alexander, *Magn. Reson. Chem.* **2005**, *43*, 776.

